ChemistryOPEN

Including Thesis Treasury

Open Access

Reprint

© Wiley-VCH Verlag GmbH & Co. KGaA, Weinheim

WILEY-VCH

A Journal of

ChemPubSoc Europe

ChemPubSoc Europe

DOI: 10.1002/open.201900345

Open Access ChemistryOPEN Full Papers

Special Issue

Mechanically-Driven Vase–Kite Conformational Switch in Cavitand Cross-Linked Polyurethanes

Martina Torelli, Francesca Terenziani, Alessandro Pedrini, Francesca Guagnini, Ilaria Domenichelli, Chiara Massera, and Enrico Dalcanale*[a]

Dedicated to Professor Jean Marie Lehn on the occasion of his 80th birthday

The eligibility of tetraquinoxaline cavitands (QxCav) as molecular grippers relies on their unique conformational mobility between a closed (*vase*) and an open (*kite*) form, triggered in solution by conventional stimuli like pH, temperature and ion concentration. In the present paper, the mechanochemical conformational switching of *ad hoc* functionalized QxCav covalently embedded in an elastomeric polydimethylsiloxane and in a more rigid polyurethane matrix is investigated. The rigid polymer matrix is more effective in converting mechanical force into a conformational switch at the molecular level, provided that all four quinoxaline wings are covalently connected to the polymer.

1. Introduction

The past few decades have seen extraordinary progress in the construction of molecular machines and switches.[1] Much effort has been devoted to the development of molecular architectures capable to perform mechanical-like movements (output) as a consequence of external stimuli (input).[2] Among the variety of switches that mimic different macroscopic objects, molecular grippers stand out for the uptake/release of molecular objects.[3] To act as a gripper, a molecule should close and open upon external stimulation to grab and release molecular objects.

Scaffolds that have emerged as particularly promising for the design of these molecular tools are tetraquinoxaline cavitands (QxCav).[4] These resorcinarene-based macrocycles are obtained through the four-fold bridging of the resorcinol scaffold with 2,3-dichloroquinoxaline moieties, which delimit a deep cavity. QxCav shows the ability to reversibly switch between two spatially well-defined conformations: an expanded *kite* (C_{2v} symmetry) and a contracted *vase* (C_{4v} symmetry), according to the position of 1,4-diazanaphtalene 'flaps', that can occupy either the equatorial or the axial positions, respectively (Figure 1).[5] Interestingly, since all intermediate conformers are energetically disfavoured, only these two discrete forms exist.[6] The energy barrier for a single flap interconversion has been estimated in 7.6 kcal mol^{-1} by DFT calculations.[7] The *vase-kite* interconversion has been extensively investigated in solution *via* different stimuli, such as pH,[8,9] temperature,[10] Zn^{2+} coordination[11,12] and redox.[3,13]

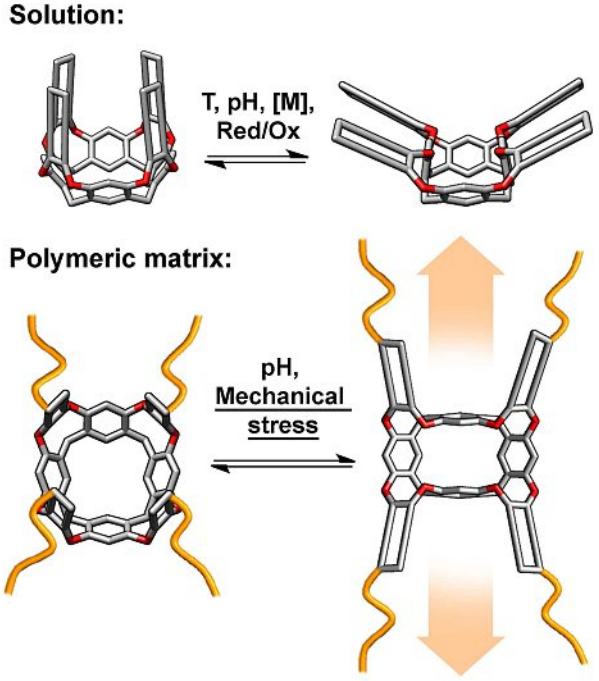

Figure 1. *Vase-kite* conformational interconversion for a generic cavitand in solution (above) and in polymeric matrix (below).

The effective integration of these molecules into functional nanodevices, however, requires a precise control of their conformation on surfaces or in the solid-state. Recently, we proved the retention of pH-driven conformational switch of QxCav covalently included in poly(butyl methacrylate) (PBMA) and polydimethylsiloxane (PDMS) matrices.[14,15]

[a] Dr. M. Torelli, Prof. F. Terenziani, Dr. A. Pedrini, Dr. F. Guagnini, Dr. I. Domenichelli, Prof. C. Massera, Prof. E. Dalcanale
Department of Chemistry, Life Sciences and Environmental Sustainability and INSTM UdR Parma
University of Parma
Parco Area delle Scienze 17/A, Parma 43124 (Italy)
E-mail: enrico.dalcanale@unipr.it

Supporting information for this article is available on the WWW under https://doi.org/10.1002/open.201900345

An invited contribution to a Special Collection dedicated to Functional Supramolecular Systems

© 2020 The Authors. Published by Wiley-VCH Verlag GmbH & Co. KGaA. This is an open access article under the terms of the Creative Commons Attribution Non-Commercial NoDerivs License, which permits use and distribution in any medium, provided the original work is properly cited, the use is non-commercial and no modifications or adaptations are made.

The incorporation of these gripper-like macrocycles in polymers paves the way for the trigger of *vase-kite* switching with unprecedented stimuli. In fact, when embedded in polymer matrices, QxCav can be considered as a "conformational" mechanophore, a term that indicates a molecule that undergoes a predictable conformational modification triggered by a mechanical force. Most of the mechanophores reported so far are characterized by the presence of strategically weakened covalent bonds, in the form of strained rings or isomerizable bonds, prone to react once mechanical forces are transferred to them from the polymer chains.[16–20] Spiropyran-based (SP) mechanophores are the most employed stress-sensitive units reported, thanks to their highly effective colour-generating nature.[21]

Over the past few years, thanks to the progress in mechanophore design, a broad range of mechanically-triggered transformations was attained.[22–28] Among these, particularly attractive are mechanophores that do not require scission of covalent bonds for the activation and change of their properties.[29–33] In the case of rotaxanes, the activation process does not involve any bond cleavage, leading to a low activation energy of the process.[30]

In the study reported herein, we extensively investigated the *vase-kite* switching of tetraquinoxaline cavitands in polymers through the application of tensile strain. To achieve this goal, we applied the tool kit of polymer mechanochemistry to induce the conformational switching.

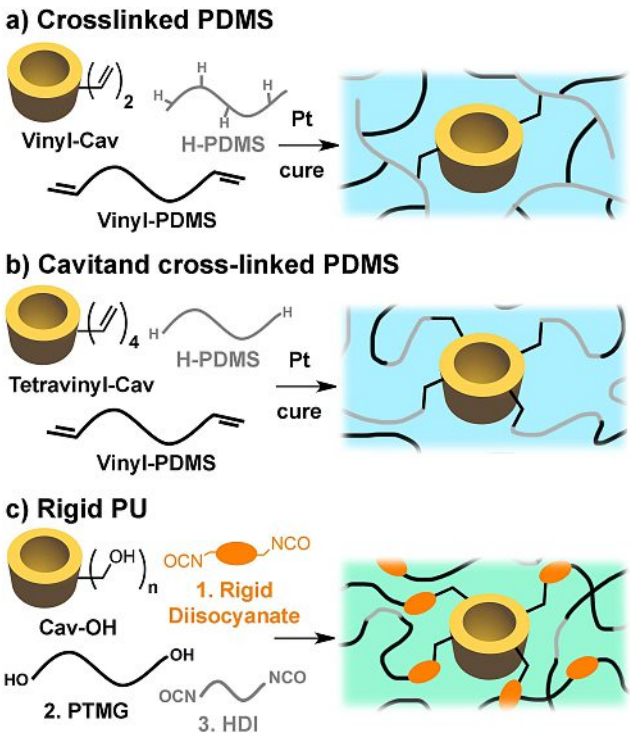

Scheme 1. PDMS (a), (L)PDMS (b), and PU (c) polymers containing covalently embedded cavitands.

2. Results and Discussion

Considering the essential role played by the nature of the polymer in terms of the efficiency of the mechanochemical transduction, we investigated two matrices (Scheme 1), an elastomeric polydimethylsiloxane (PDMS) and a more rigid polyurethane (PU).

Tetraquinoxaline cavitands were obtained *via* a convergent approach where either functionalized or non-functionalized quinoxalines were introduced on resorcinarenes or partially bridged cavitands. Since DFT calculations on cavitands suggested that all intermediate states between the two discrete conformers are energetically disfavoured, we initially assumed that the application of a tensile force to two quinoxaline wings in distal position would elicit the opening of the other two, thus promoting the *vase-kite* interconversion. Based on this hypothesis, we performed the synthesis of distal-difunctionalized tetraquinoxaline cavitands bearing suitable moieties for the covalent incorporation into the polymeric network. In particular, terminal vinyl groups were introduced to ensure the embedding into the PDMS matrix, while hydroxy groups were exploited for the PU one. The anchoring site for polymer grafting was connected to the cavitand core *via* easily accessible ester linkages and through aliphatic spacers, in order to prevent a possible decrease in reactivity for steric effects. Moreover, since any modification at the upper rim walls might destabilize the *vase* conformation, we exclusively functionalized the quinoxaline walls in position 6 or 7, thus minimizing steric hindrance.

For both matrices, specimens with the corresponding tetrafunctionalized cavitand were prepared and mechanically tested, in the hypothesis that the use of a QxCav molecule acting as cross-linker into the polymer could result in a more efficient channelling of the applied force to the mechanophore unit. Also in this case, cavitand walls decoration was performed *via* a convergent approach through a bridging reaction with pre-functionalized 2,3-dichloroquinoxalines.

The above-described cavitands were employed as co-monomers in the preparation of polymer specimens. Furthermore, in order to irrefutably correlate the applied mechanical stimulus to the desired response, excluding any other possible activation mechanism (e.g. thermal activation), the corresponding control specimens, with physically dispersed, mono- or non-quinoxaline anchored QxCav, were prepared and mechanically tested.

2.1. Alkene-Functionalized Cavitands for PDMS

As demonstrated by Craig and co-workers,[34] polysiloxanes are suitable matrices for mechanochemical applications since, besides their well-known high stretchability and mechanical strength, they present an efficient transduction of applied forces to embedded mechanophore units. The conventional protocol for the covalent incorporation of stress-responsive

© 2020 The Authors. Published by Wiley-VCH Verlag GmbH & Co. KGaA

elements into PDMS relies on hydrosilylation reaction, requiring the presence of terminal double bonds.

Accordingly, cavitand **C2A** (Scheme 2), bearing two distal alkenyl groups suitable for mechanochemical transduction, was prepared following a previously described procedure.[14] Monofunctionalized cavitand **C1A** was synthesized by bridging ω-decene-2,3-dichloroquinoxaline **1**[14] on the corresponding triquinoxaline scaffold, obtained from the unsubstituted QxCav $\mathbf{C_V}$ by selective monoquinoxaline excision reaction with catechol under basic conditions.[35] The four-fold bridging of dichloroquinoxaline on a resorcinarene scaffold afforded the tetrafunctionalized QxCav **C4A** as racemic mixture of two enantiomers with C_4 symmetry. This regioselectivity can be explained with steric effects; in fact, after the first statistical bridging event, hindrance of the introduced aliphatic chain influences the following insertions, thus leading to the functionalization in alternate positions at expense of the overall yield. The high symmetry, revealed by very sharp signals in the ^{1}H NMR spectrum, was unambiguously confirmed by single crystal X-ray diffraction (Figure S1). To provide an analogous cross-linker in control films, QxCav $\mathbf{C4A_L}$, bearing four double bonds at the lower rim, was synthetized adapting previously reported procedures.[36,37]

Compounds **C1A**, **C4A** and $\mathbf{C4A_L}$ were characterized by ^{1}H NMR and MALDI-TOF spectrometry. NMR spectroscopy is diagnostic of cavitand conformation; indeed, it is widely reported in the literature[4] that the resonance of methine protons in solution is highly conformation-dependent, with a difference in chemical shift of more than 2 ppm between *vase* ($\approx$5.6 ppm) and *kite* ($\approx$3.9 ppm). Thus, the presence of a signal at around 5.6 ppm in all cases confirmed the retention of the *vase* conformation. Finally, cavitand $\mathbf{C_K}$, bearing four methyl groups in apical position that force it in *kite* conformation by steric effects, was synthesized according to previously reported procedures.[38]

2.2. PDMS Functionalization and Mechanical Tests

RTV 615, the selected matrix for PDMS specimens, is a two component (base and curing agent, typically mixed in a 10:1 ratio) silicone elastomer comprising of vinyl terminated poly (dimethylsiloxane), poly(methylhydrosiloxane-codimethyl siloxane) copolymer and a platinum catalyst. QxCav **C1A**, **C2A**, **C4A** and $\mathbf{C4A_L}$ were covalently incorporated into the matrix *via* hydrosilylation protocol to give specimens **PDMS-C1A**, **PDMS-C2A**, **PDMS-C4A** and $\mathbf{PDMS\text{-}C4A_L}$, respectively (Table S2, concentrations from 0.05 to 0.7 % w/w). Effective covalent embedding was confirmed by Soxhlet extraction with chloroform, performed on **PDMS-C2A** as representative (Figure S2a). The extracted polymer and the organic phase were analysed by UV-Vis spectroscopy: the absorption pattern of the cavitand was observed only in the polymeric specimen, while it was not present in the organic phase. This experiment, although being crucial for proving the covalent incorporation of cavitands in the polysiloxane network, does not demonstrate the effective reaction of all their functionalities. Unfunctionalized QxCav $\mathbf{C_V}$ and $\mathbf{C_K}$, instead, were physically dispersed in PDMS; the resulting $\mathbf{PDMS\text{-}C_V}$ and $\mathbf{PDMS\text{-}C_K}$ specimens provided a reference of the two conformers in the matrix (Table S3). In this case Soxhlet extraction with chloroform caused the almost complete removal of dispersed cavitands from the specimens, as evidenced by the UV-Vis spectra of the two phases (Figure S2b).

Comparison between the UV-Vis spectra of $\mathbf{C_V}$ and $\mathbf{C_K}$ in solution and in PDMS revealed the retaining of the optical properties at the solid state, with two maxima of absorption at 318 and 330 nm for *vase* QxCav, and at 335 and 348 nm for the *kite* form (Figure S3). Moreover, UV-Vis spectroscopy was already used to confirm the protonation-driven interconversion for **PDMS-C2A**, suggesting that, even when covalently embedded into the polymer matrix, cavitands possess enough free volume to open up into the *kite* conformation.[14] In this work, cavitands interconversion upon tensile stress was tested. Specimens containing mono- and di-functionalized QxCav **C1A** and **C2A** at different concentrations were uniaxial stretched and UV-Vis spectra were recorded at progressively increasing applied force (Figure 2).

In particular, **PDMS-C1A** samples were tested to isolate the effects of bidirectional strain. In all cases, no maxima variation was observed. Figure 3a, showing the experiment for **PDMS-C2A**, is representative of the general behavior observed for all tested specimens. Since the only visible effect is the λ-independent decrease in absorbance due to the thinning of polymer films upon elongation, we can conclude that the visual monitoring of *vase-kite* force-induced switching *via* UV-Vis spectroscopy was not possible.

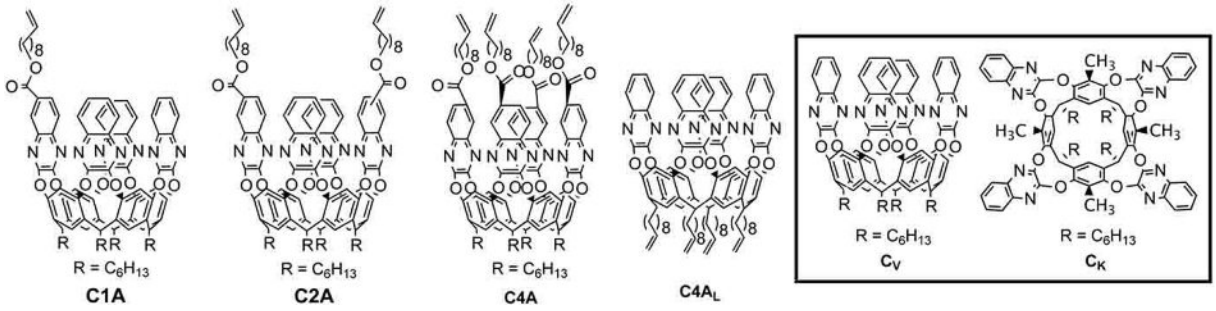

Scheme 2. Overview of alkene functionalized employed in PDMS polymers preparation. Unsubstituted cavitands, reported in the inset, have been prepared as reference compounds.

© 2020 The Authors. Published by Wiley-VCH Verlag GmbH & Co. KGaA

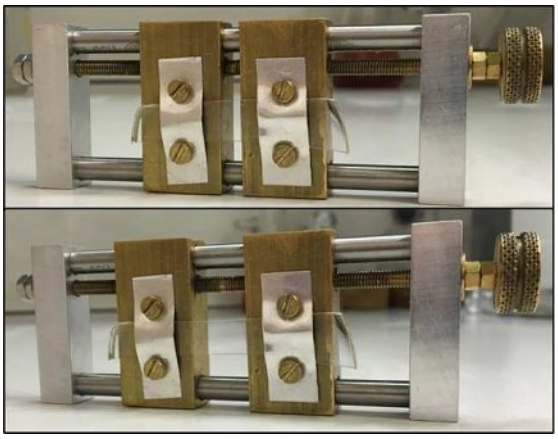

Figure 2. Digital photographs of the device employed for mechanical tests: relaxed sample (top) and loaded sample at 300% stretching (bottom).

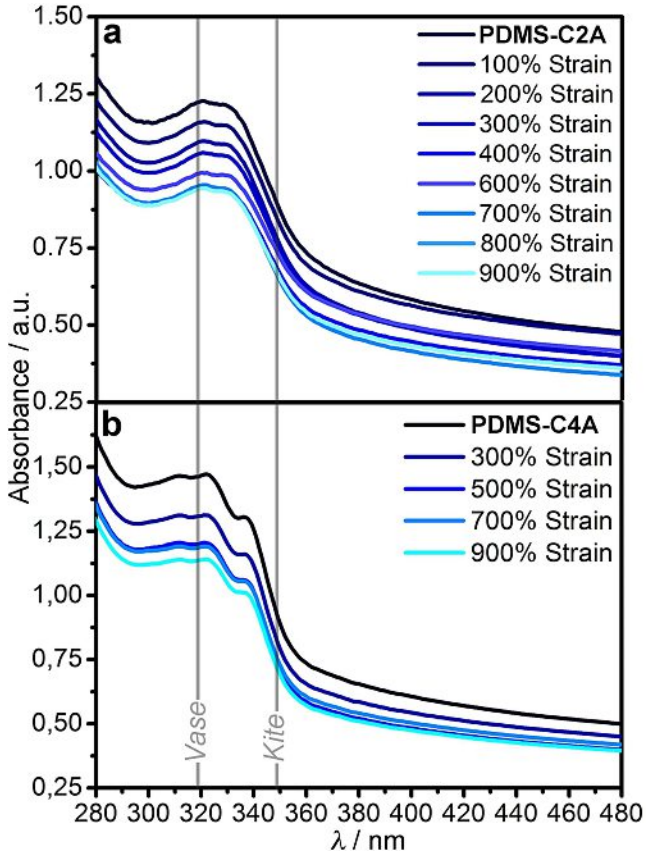

Figure 3. UV-Vis spectra of (a) **PDMS-C2A** (0.5% w/w, Table S2 entry V) and (b) **PDMS-C4A** (0.3% w/w, Table S2 entry X) upon progressive elongation. Vertical grey lines correspond to maxima in UV-Vis spectra for $CHCl_3$ solution of *vase* and *kite* conformers.

To test the hypothesis that all four quinoxaline wings need to be stretched in order to induce interconversion, active and control specimens with tetrafunctionalized QxCav **C4A** and **C4A$_L$**, respectively, were prepared. Unlike QxCav **C4A**, cavitand **C4A$_L$**, bearing the anchoring sites at the lower rim, is not expected to be affected by any conformational change upon stretching (Figure S4). The UV-Vis spectrum of cavitand **C4A** in solution shows a slightly shifted maximum (323 nm instead of 318 nm for QxCav **C$_V$**), while the diagnostic shoulder attributed to the protonated *kite* form remained unaltered after functionalization (Figure S5). **PDMS-C4A** specimens were uniaxially stretched; once again, UV-Vis spectra recorded at progressively increasing applied force did not show any maxima variation upon elongation (Figure 3b). Considering the high number of cross-linking sites in pristine elastomeric PDMS, we supposed that the unresponsiveness of our system could be justified by a complete or partial prevention in the transmission of mechanical energy to the mechanophore.

In order to maximize the channelling of tensile force to the cavitand, we modified the polymer backbone by replacing the conventional RTV 615 curing agent, consisting of the poly (methylhydrosiloxane-codimethylsiloxane) copolymer acting as cross-linker, with a ditopic H-terminated-poly (dimethylsiloxane). Thus, in the resulting polymer **(L)PDMS-C4A**, the unique cross-linking agent is represented by tetrafunctionalized cavitand **C4A**. Different polymeric samples were prepared, both varying the ratio between vinyl-terminated and H-terminated pre-polymers and the amount of cross-linker (Table S4), to find the optimal conditions in terms of mechanical properties of the resulting specimens. Tetra-ω-alkene functionalized QxCav **C4A$_L$**, bearing double bonds at the lower rim, was used as cross-linker in the preparation of control specimens **(L)PDMS-C4A$_L$**, in order to provide a reticulation similar to the active ones. Mechanical testing on **(L)PDMS-C4A** failed to evidence a clear maxima variation in the UV-Vis spectra, although an increase in the absorbance at 335 nm was observed against the trend of thinning of the specimen upon elongation (Figure 4a). Interestingly, the apparent increase in the adsorbance, occurring at the wavelength of the first maxima for the *kite* conformer, was not observed in control specimens **(L)PDMS-C4A$_L$** (Figure 4b).

A mechanically-driven *vase-kite* interconversion for PDMS-embedded QxCav was not clearly detected. A possible reason could be the low degree of force-elicited conversion, already reported for other mechanophores,[39–41] which makes the detection of cavitands conformational switching *via* UV-Vis spectroscopy very difficult with respect to a visible colour change. Thus, a more efficient system ensuring a higher degree of conversion for the mechanophore unit is needed. Therefore, we decided to replace the elastomeric PDMS with a more rigid matrix, such as PU.

2.3. Hydroxyl Functionalized Cavitands for PU

Following a protocol reported in the literature,[41] the covalent inclusion of cavitands in PU matrix was obtained *via* step growth polymerization. The mechanophore units used for this study are summarised in Scheme 3. In particular, mono-ω-hydroxy QxCav **C1H** and bis-ω-hydroxy QxCav **C2H** were employed as co-monomers in the step growth polymerization, while tetra-ω-hydroxy QxCav **C4H** acts as cross-linker in active specimens. Finally, tetra-ω-hydroxy velcrand **C$_K$4H** was designed as a reference for the covalently embedded *kite* form into PU. The convergent synthetic approach, analogously to the pre-

© 2020 The Authors. Published by Wiley-VCH Verlag GmbH & Co. KGaA

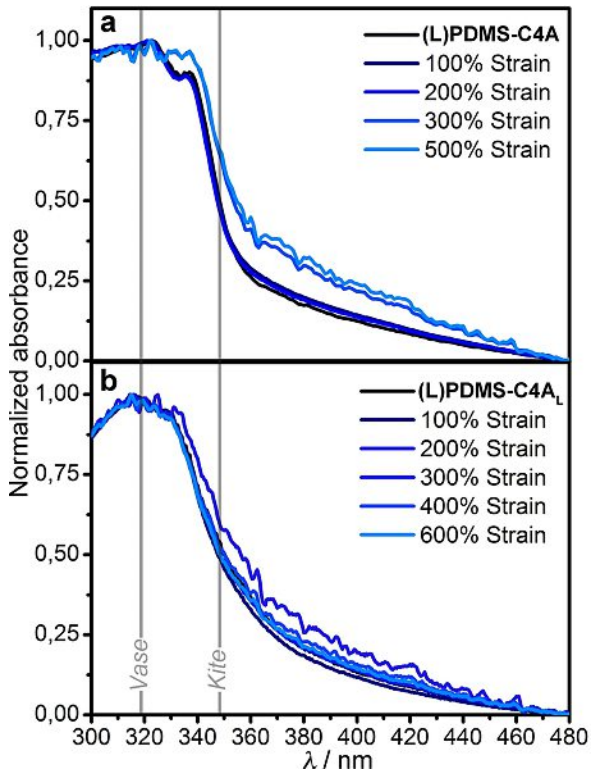

Figure 4. Normalized UV-Vis spectra of (a) **(L)PDMS-C4A** (1% w/w, Table S4 entry VI) and (b) **(L)PDMS-C4A$_L$** (1% w/w, Table S4 entry IX) upon progressive elongation. Vertical grey lines correspond to maxima in UV-Vis spectra for $CHCl_3$ solution of *vase* and *kite* conformers.

vious one, was based on the bridging reaction of *ad hoc* functionalized dichloroquinoxalines onto variously substituted cavitand scaffolds. In detail, 2,3-dichloroquinoxaline **2**, bearing a hydroxy group protected as *tert*-butyl dimethyl silyl ether (TBDMS), was prepared from the easily accessible 2,3-dichloroquinoxaline-6-carbonyl chloride through a convenient acyl substitution with mono-protected hexanediol under mild conditions. Nucleophilic substitution of **2** by triquinoxaline and AC-diquinoxaline QxCav hydroxyl groups, followed by deprotection of the TBDMS group, afforded respectively cavitands **C1H** and **C2H**, suitable for the covalent incorporation in PU (see SI for the detailed synthetic procedures). Tetrafunctionalized cavitand **C4H**, designed for acting as unique cross-linker in the linear polymer network, was obtained by the four-fold bridging of the corresponding resorcinarene with **2**, under microwave irradiation, and subsequent deprotection. The high resolution of ^{1}H NMR signals for **C4H** confirmed that, also in this case, only the two enantiomers bearing alkyl functionalities in alternate positions were obtained. This regioselectivity, due to steric effects, justifies the low yield of the bridging reaction. Finally, QxCav **C$_K$4H**, forced in the *kite* conformation, was obtained from the corresponding resorcinarene scaffold *via* four-fold bridging of **2** and subsequent deprotection. Unlike QxCav **C4H**, the broad signals in the ^{1}H NMR spectra suggest that both cavitand **C$_K$4H** and its TBDMS-protected precursor **6** were obtained as an inseparable mixture of constitutional isomers. The lack of regioselectivity for the bridging reaction is probably due to the expanded conformation of the resulting QxCav, where the absence of steric effects does not impose any geometrical constraint to the subsequent insertions of dichloroquinoxaline **2**.

2.4. PU Functionalization and Mechanical Tests

The selected matrix is a relatively rigid polymer obtained by step growth polymerization between poly(tetramethylene glycol) (PTMG, Mn = 1000) and isophorone diisocyanate, followed by the addition of hexamethylene diisocyanate (HDI) as chain extender. The use of isophorone instead of the more common methylene diisocyanate meets the need of optical transparency for the resulting films, thus facilitating the visualization of *vase-kite* switching *via* optical spectroscopy.

Firstly, unfunctionalized QxCav **C$_V$** and **C$_K$** were physically dispersed in the polymer and the resulting specimens **PU-C$_V$** and **PU-C$_K$** provided a reference of the two conformers in the solid state. UV-Vis spectroscopy confirmed that the optical properties are essentially retained when moving from solution to the solid state (Figure S7). QxCav **C1H**, **C2H**, **C4H** and **C$_K$4H** bearing hydroxy groups, were employed as co-monomers in the step growth polymerization. Thus, tetra-ω-hydroxy functionalized QxCav **C4H** was employed in the preparation of force-responsive films **PU-C4H**, while functionalized QxCav **C1H**, **C2H** and **C$_K$4H**, together with QxCav **C$_V$**, were used for control films **PU-C1H**, **PU-C2H**, **PU-C$_K$4H** and **PU-C$_V$** (Table S5-S6, concentrations from 0.01 to 0.5% w/w). Differential scanning calorimetry (DSC) analysis performed on **PU-C4H** (Figure S6) revealed a glass transition temperature (T_g) of −36 °C.

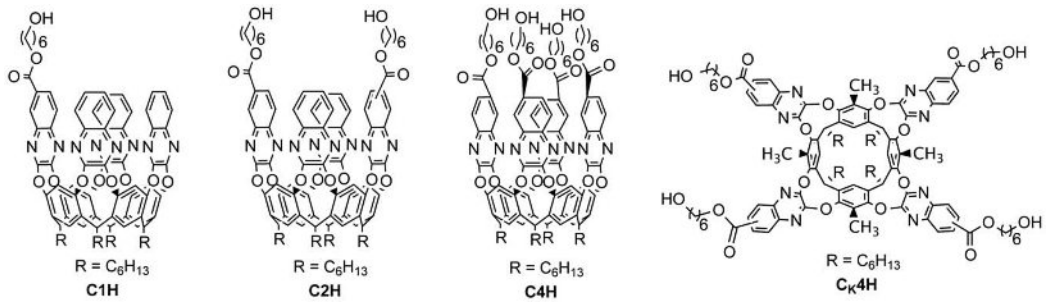

Scheme 3. Overview of hydroxy functionalized cavitands employed in PU polymers preparation.

© 2020 The Authors. Published by Wiley-VCH Verlag GmbH & Co. KGaA

Cavitands interconversion upon mechanical stress was tested *via* UV-Vis absorption spectroscopy. The stretching of **PU-C4H** induces the rise of a shoulder at 348 nm, corresponding to the second maximum of the kite conformer. Figure 5a, illustrating the experiment for **PU-C4H** (0.3% w/w, Table S5 entry VII), is representative of the general behaviour observed for all tested specimens, where changes in the UV-Vis spectra become sizable for a degree of stretching of about 200%. The same mechanical tests performed on control specimens failed to evidence comparable changes in the UV-Vis spectra (Figure S8); Figure 5b, showing the spectra recorded for **PU-C$_V$** upon elongation, resumes the general behaviour observed for all control samples (Figure S9 and S10).

In order to confirm unambiguously the occurrence of the mechanically-triggered conformational switching, fluorescence measurements were performed. Preliminary studies in solution on QxCav **C$_V$** and **C$_K$** suggested a solvatochromic nature of the emission band, which redshifts with increasing solvent polarity (Figure S11). When dissolved in solvents of medium-high polarity, the fluorescence band of the *vase* conformer is located at roughly the same position as the band of the *kite* conformer, in low-polarity solvents the band of the *vase* is located at shorter wavelengths. This suggests that, in low-polarity solvents, the fluorophoric units in the *vase* conformer are less solvated than in the *kite* conformer. This can be rationalized assuming the formation of an 'intramolecular quadrimer' in the contracted conformer. Analogous behaviour was observed comparing **PU-C$_V$** with **PU-C$_K$** and **PU-C4H** with **PU-C$_K$4H** (Figure S12): in both cases, the emission band of the *vase* conformer is blue shifted with respect to the *kite* one (15 nm and 30 nm, respectively), suggesting that the *vase* conformer is less solvated than the *kite* one also in the solid state. Remarkably, while the contracted form shows a redshift of 10 nm when passing from being physically dispersed (**PU-C$_V$**) to being covalently linked to the polymeric network (**PU-C4H**), the expanded one moves of 30 nm (**PU-C$_K$** vs **PU-C$_K$4H**). This observation, supported by concentration dependence studies in solution (Figure S13), strongly suggests that the *kite* compound, when dispersed, tends to form intermolecular aggregates, resulting in an emission behaviour closer to the 'intramolecular quadrimer' situation showed by the *vase* compound in low-polarity media. On the other hand, covalent embedding into the polymeric structure prevents the formation of intermolecular aggregates, leading to an emission behaviour more similar to the one observed in medium-high polarity solvents. By contrast, the aggregation effect for the *vase* conformer is essentially non-influenced by the nature of cavitand incorporation into PU, having mainly an intramolecular origin.

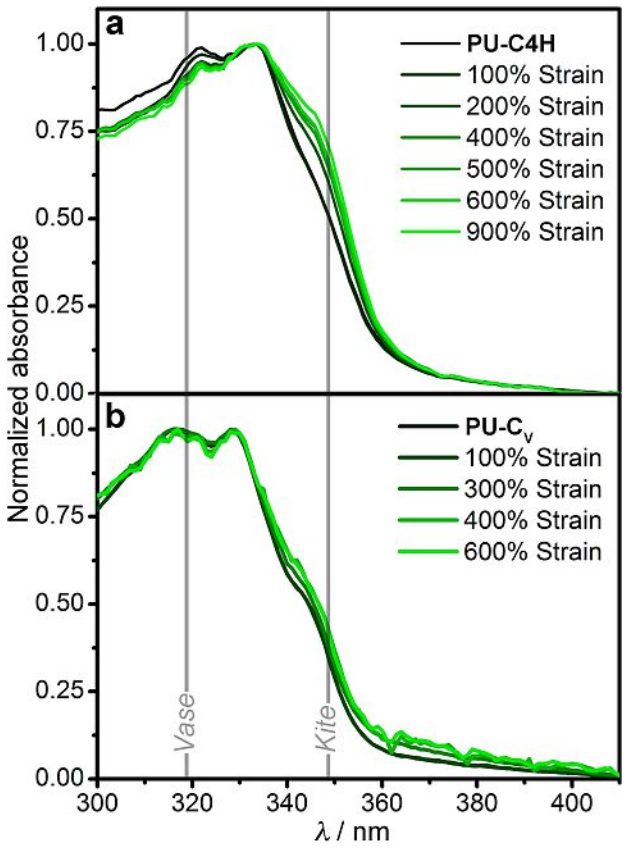

Figure 5. Normalized UV-Vis spectra of (a) **PU-C4H** (0.3% w/w, Table S5 entry VII) and (b) **PU-C$_V$** (0.3% w/w, Table S6 entry II) upon progressive elongation. Vertical grey lines correspond to maxima in UV-Vis spectra for $CHCl_3$ solution of *vase* and *kite* conformers.

Once verified that the four-fold opening of the quinoxaline wings leads to a bathochromically-shifted emission in PU, mechanical tests on **PU-C4H** were performed. Because of the thinning of the stretched specimens, a quantitative evaluation of the absolute emission intensity upon interconversion was considered unreliable. Thus, only the shape of the emission spectra is discussed. As expected, emission spectra of control films **PU-C$_V$** did not reveal any significant change upon elongation (Figure S14); by contrast, in agreement with UV-Vis measurements, a change in the emission profile for **PU-C4H** was observed (Figure 6a).

Interestingly, mechanical tests performed on several specimens pointed out a different behaviour. Figure 6a resumes the most common behaviour observed in active films: the emission spectrum of the pristine film (black thick line) shows a single maximum at 390 nm and, upon stretching, the emission band broadens in the long-wavelength side, with a 10-nm redshift of the maximum (green thick line). A few specific specimens, instead, have an emission spectrum showing two maxima already for the pristine film: a main band at 390 nm and a strong shoulder at about 440 nm (Figure 6b, black thick line). This shoulder becomes the most intense band under tensile stress (green thick line in Figure 6b).

Deconvolution of the emission spectra (on the frequency scale) with Gaussian lines was performed, starting from the spectra in Figure 6b. The emission band of the pristine film (black thick line) is nicely fitted as the sum of two Gaussian functions (thin black line). The two deconvoluted components, the green dashed area for the *vase* and the grey area for the *kite* conformer, have a clear resemblance with the emission spectra of **PU-C$_V$** blue line in Figure 6c) and **PU-C$_K$4H** (red line in Figure 6c), respectively. In order to fit the emission spectrum of the stretched film (green thick line), the position and width of the two Gaussians were kept fixed and only their relative

© 2020 The Authors. Published by Wiley-VCH Verlag GmbH & Co. KGaA

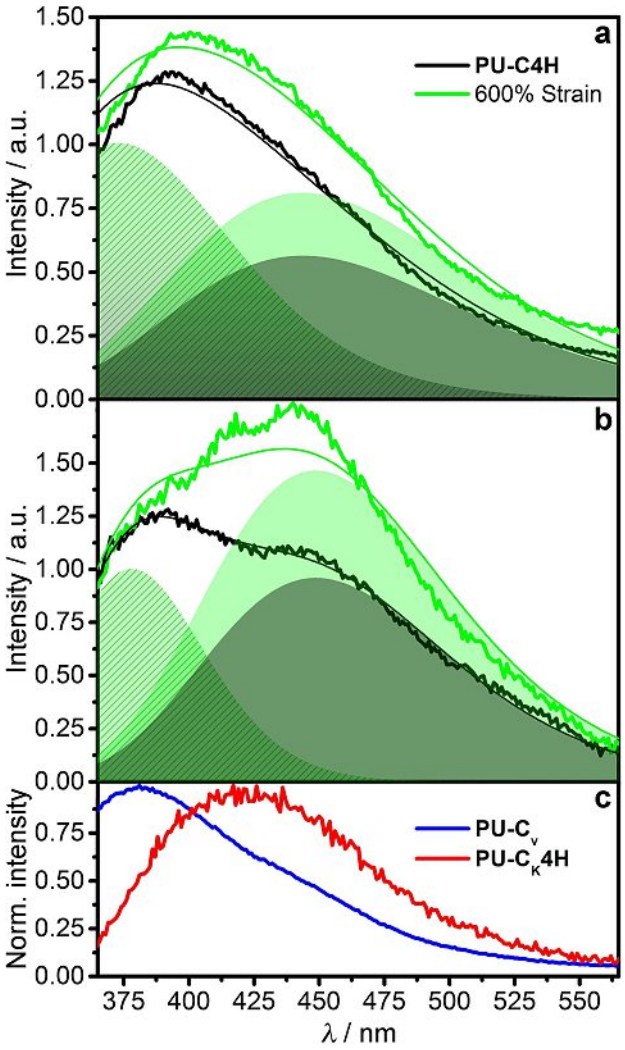

Figure 6. a) Emission spectra representative of the most common behaviour observed for **PU-C4H** (0.01% w/w, Table S5 entry X) upon tensile elongation (thick black and red lines). Fitting of the curves (results as thin black and green lines) as sums of two Gaussian bands (filled areas, dashed for the *vase* and solid for the *kite* conformers). b) Same as panel a, but reporting the behaviour of a few selected specimens. c) Emission spectra of **PU-C$_V$** (0.01% w/w, Table S6 entry III, blue line) and **PU-C$_K$4H** (0.01% w/w, Table S5 entry XII, red line), reported as references.

intensity was varied, obtaining the green thin line as the best fit. In this way, we estimated a relative increase of the long-wavelength band (green area) of a factor amounting to 1.53. The same analysis was performed on experimental spectra in Figure 6a; since in this case the two components of the emission band are more difficult to recognize, we chose to fix the position of the two Gaussian lines as extracted from the previous fitting, while allowing the optimization of their width and intensity. In this case, analogously to the previous one, a relative increase of the long-wavelength band of about a 1.44 factor was estimated upon tensile elongation. Therefore, for all the specimens, two components in the fluorescence spectrum can be recognized, one corresponding to the emission of the contracted form **PU-C$_V$** and the other, strongly redshifted, similar to the emission of the expanded form cross-linked in the polymeric network, **PU-C$_K$4H**. The relative contribution of this latter band clearly increases under tensile stress, proving the occurrence of the mechanochemical interconversion. The deconvolution analysis suggests that a certain amount of *kite* structure is already present in the pristine films; a likely explanation can rely on the nature of the chosen matrix, whose rigidity exerts, during the polymerization process, enough tension on cavitand molecules to induce a partial *vase-kite* interconversion. For most of the samples (case exemplified in Figure 6a), an about 30% contribution of the open conformation is already recognized in the pristine films, while in a few specific samples (Figure 6b) this contribution amounts to about 50%. In all cases, however, upon a mechanical solicitation, the open component increases of a relative factor of about 1.5.

3. Conclusions

In conclusion, two different polymeric matrices were investigated for promoting the *vase-kite* interconversion of tetraquinoxaline cavitands *via* mechanochemical stimulus. Elastomeric PDMS, despite being known for the successful activation of spiropyran mechanophores,[34,42,43] failed to evidence any maxima variation *via* UV-Vis spectroscopy for both di- and tetrafunctionalized cavitands. The use of a more rigid PU matrix, together with the incorporation of tetrafunctionalized QxCav units as unique cross-linkers into the polymeric network, resulted in the expected responsiveness upon tensile elongation, detected both *via* UV-Vis and fluorescence spectroscopy. Considering the lack of any significant spectroscopic variation for control specimens, we conclude that the observed response can be traced back to a mechanically induced conformational change of QxCav units embedded into the PU matrix, even if not all the cavitands reacted to the mechanical stimuli. Moreover, experimental data suggest that, contrary to the initial suppositions, all four quinoxaline wings need to be covalently anchored to the polymer backbone in order to experience an efficient transduction of tensile stress. Furthermore, fluorescence spectra allowed a preliminary quantification of the degree of activation in terms of relative increase in the intensity of the long-wavelength band.

Experimental Section

Detailed experimental procedures, characterization of all new compounds and spectroscopic investigation of polymeric specimens are available in the Supporting Information (SI).

PDMS Samples Preparation

RTV 615 base (3.0 g) and a THF cavitand solution were homogenized with a Vortex in a 15 mL Falcon tube. RTV 615 curing agent (0.3 g) was added, and the tube was extensively shaken with a Vortex. The homogenous mixture was degassed under vacuum and poured onto a PTFE plate. After a second degassing, the sample was cured in an oven at 60 °C for 16 h. Once cured the film was peeled away and cut into stripes for testing.

© 2020 The Authors. Published by Wiley-VCH Verlag GmbH & Co. KGaA

(L)PDMS Samples Preparation

RTV 615 base and a THF cavitand solution were homogenized with a Vortex in a 15 mL Falcon tube. Ditopic H-terminated PDMS (RTV 615 Base/H term. PDMS ratios reported in Table S4) and Karstedt's catalyst were added, and the tube was extensively shaken with a Vortex. The homogenous mixture was degassed under vacuum and poured onto a PTFE plate. After a second degassing, the sample was cured in an oven at 60 °C for 16 h. Once cured the film was peeled away and cut into stripes for testing.

PU Samples Preparation

A solution of isophorone diisocyanate (59 eq.) in dry THF was slowly added to a solution of cavitand and DABCO (8.42 eq.) in dry THF. The mixture was stirred at 60 °C for 2 h. The solution was cooled at room temperature and added to a solution of poly(tetramethylene glycol) (M_w 1000; 1216 eq.) and DABCO (1.05 eq.) in dry THF. The mixture was stirred under vacuum and heated at 50 °C to remove volatiles. After the addition of hexamethylene diisocyanate (1180 eq.), the viscous pre-polymer was degassed under vacuum and poured onto a PTFE plate. After a second degassing, the sample was cured in an oven for 48 h at 60 °C and for 48 h at room temperature before testing. Once cured, the film was peeled away and cut into stripes

Acknowledgements

The authors thank Dr. Gianluca Paredi of SITEIA, University of Parma, for high-resolution MALDI-TOF analyses. We thank Elantas Europe for providing samples of RTV 615. A.P. thanks INSTM for support of his fellowship. This work has benefited from the equipment and framework of the COMP-HUB Initiative, funded by the 'Departments of Excellence' program of the Italian Ministry for Education, University and Research (MIUR, 2018-2022).

Keywords: cavitands · conformational mechanophores · polyurethane · polydimethylsiloxane · molecular grippers

[1] B. L. Feringa, W. R. Browne, Eds., *Molecular Switches*, Wiley-VCH Verlag GmbH & Co. KGaA, Weinheim, Germany, **2011**.
[2] B. L. Feringa, *Angew. Chem. Int. Ed.* **2017**, *56*, 11060–11078; *Angew. Chem.* **2017**, *129*, 11206–11226.
[3] J. V. Milić, F. Diederich, *Chem. Eur. J.* **2019**, *25*, 8440–8452.
[4] J. R. Moran, S. Karbach, D. J. Cram, *J. Am. Chem. Soc.* **1982**, *104*, 5826–5828.
[5] V. A. Azov, A. Beeby, M. Cacciarini, A. G. Cheetham, F. Diederich, M. Frei, J. K. Gimzewski, V. Gramlich, B. Hecht, B. Jaun, *Adv. Funct. Mater.* **2006**, *16*, 147–156.
[6] D. F. Hahn, J. V. Milić, P. H. Hünenberger, *Helv. Chim. Acta* **2019**, *102*, e1900060.
[7] I. Pochorovski, Redox-Switchable Cavitands: Conformational Analysis and Binding Studies, Ph.D. Thesis, ETH-Dissertation Nr. 21351, ETH Zürich, **2013**.
[8] P. J. Skinner, A. G. Cheetham, A. Beeby, V. Gramlich, F. Diederich, *Helv. Chim. Acta* **2001**, *84*, 2146–2153.
[9] P. Pagliusi, F. Lagugné-Labarthet, D. K. Shenoy, E. Dalcanale, Y. R. Shen, *J. Am. Chem. Soc.* **2006**, *128*, 12610–12611.
[10] J. R. Moran, J. L. Ericson, E. Dalcanale, J. A. Bryant, C. B. Knobler, D. J. Cram, *J. Am. Chem. Soc.* **1991**, *113*, 5707–5714.
[11] P. Amrhein, A. Shivanyuk, D. W. Johnson, J. Rebek, *J. Am. Chem. Soc.* **2002**, *124*, 10349–10358.
[12] M. Frei, F. Marotti, F. Diederich, *Chem. Commun.* **2004**, *10*, 1362–1363.
[13] I. Pochorovski, F. Diederich, *Acc. Chem. Res.* **2014**, *47*, 2096–2105.
[14] M. Torelli, I. Domenichelli, A. Pedrini, F. Guagnini, R. Pinalli, F. Terenziani, F. Artoni, R. Brighenti, E. Dalcanale, *Synlett* **2018**, *29*, 2503–2508.
[15] R. Brighenti, F. Artoni, F. Vernerey, M. Torelli, A. Pedrini, I. Domenichelli, E. Dalcanale, *J. Mech. Phys. Solids* **2018**, *113*, 65–81.
[16] C. L. Brown, S. L. Craig, *Chem. Sci.* **2015**, *6*, 2158–2165.
[17] J. Li, C. Nagamani, J. S. Moore, *Acc. Chem. Res.* **2015**, *48*, 2181–2190.
[18] S. Akbulatov, R. Boulatov, *ChemPhysChem* **2017**, *18*, 1418.
[19] N. Willis-Fox, E. Rognin, T. A. Aljohani, R. Daly, *Chem* **2018**, *4*, 2499–2537.
[20] R. W. Barber, M. E. McFadden, X. Hu, M. J. Robb, *Synlett* **2019**, *30*, 1725–1732.
[21] M. Li, Q. Zhang, Y. N. Zhou, S. Zhu, *Prog. Polym. Sci.* **2018**, *79*, 26–39.
[22] C. R. Hickenboth, J. S. Moore, S. R. White, N. R. Sottos, J. Baudry, S. R. Wilson, *Nature* **2007**, *446*, 423–427.
[23] D. A. Davis, A. Hamilton, J. Yang, L. D. Cremar, D. Van Gough, S. L. Potisek, M. T. Ong, P. V. Braun, T. J. Martínez, S. R. White, *Nature* **2009**, *459*, 68–72.
[24] A. Piermattei, S. Karthikeyan, R. P. Sijbesma, *Nat. Chem.* **2009**, *1*, 133–137.
[25] J. M. Lenhardt, M. T. Ong, R. Choe, C. R. Evenhuis, T. J. Martinez, S. L. Craig, *Science.* **2010**, *329*, 1057–1060.
[26] Y. Chen, A. J. H. Spiering, S. Karthikeyan, G. W. M. Peters, E. W. Meijer, R. P. Sijbesma, *Nat. Chem.* **2012**, *4*, 559–562.
[27] A. G. Tennyson, K. M. Wiggins, C. W. Bielawski, *J. Am. Chem. Soc.* **2010**, *132*, 16631–16636.
[28] M. B. Larsen, A. J. Boydston, *J. Am. Chem. Soc.* **2013**, *135*, 8189–8192.
[29] G. A. Filonenko, J. A. M. Lugger, C. Liu, E. P. A. van Heeswijk, M. M. R. M. Hendrix, M. Weber, C. Müller, E. J. M. Hensen, R. P. Sijbesma, E. A. Pidko, *Angew. Chem. Int. Ed.* **2018**, *57*, 16385–16390.
[30] Y. Sagara, M. Karman, E. Verde-Sesto, K. Matsuo, Y. Kim, N. Tamaoki, C. Weder, *J. Am. Chem. Soc.* **2018**, *140*, 1584–1587.
[31] T. Yamakado, K. Otsubo, A. Osuka, S. Saito, *J. Am. Chem. Soc.* **2018**, *140*, 6245–6248.
[32] T. Muramatsu, Y. Sagara, H. Traeger, N. Tamaoki, C. Weder, *ACS Appl. Mater. Interfaces* **2019**, *11*, 24571–24576.
[33] Y. Sagara, M. Karman, A. Seki, M. Pannipara, N. Tamaoki, C. Weder, *ACS Cent. Sci.* **2019**, *5*, 874–881.
[34] G. R. Gossweiler, G. B. Hewage, G. Soriano, Q. Wang, G. W. Welshofer, X. Zhao, S. L. Craig, *ACS Macro Lett.* **2014**, *3*, 216–219.
[35] P. P. Castro, G. Zhao, G. A. Masangkay, C. Hernandez, L. M. Gutierrez-Tunstad, *Org. Lett.* **2004**, *6*, 333–336.
[36] E. U. T. van Velzen, J. F. J. Engbersen, D. N. Reinhoudt, *Synthesis* **1995**, *8*, 989–997.
[37] G. G. Condorelli, A. Motta, M. Favazza, I. L. Fragalà, M. Busi, E. Menozzi, E. Dalcanale, L. Cristofolini, *Langmuir* **2006**, *22*, 11126–11133.
[38] D. J. Cram, H. J. Choi, J. A. Bryant, C. B. Knobler, *J. Am. Chem. Soc.* **1992**, *114*, 7748–7765.
[39] J. M. Lenhardt, A. L. Black, B. A. Beiermann, B. D. Steinberg, F. Rahman, T. Samborski, J. Elsakr, J. S. Moore, N. R. Sottos, S. L. Craig, *J. Mater. Chem.* **2011**, *21*, 8454–8459.
[40] M. B. Larsen, A. J. Boydston, *J. Am. Chem. Soc.* **2014**, *136*, 1276–1279.
[41] C. K. Lee, D. A. Davis, S. R. White, J. S. Moore, N. R. Sottos, P. V. Braun, *J. Am. Chem. Soc.* **2010**, *132*, 16107–16111.
[42] G. R. Gossweiler, C. L. Brown, G. B. Hewage, E. Sapiro-Gheiler, W. J. Trautman, G. W. Welshofer, S. L. Craig, *ACS Appl. Mater. Interfaces* **2015**, *7*, 22431–22435.
[43] C. L. Brown, M. H. Barbee, J. H. Ko, H. D. Maynard, S. L. Craig, *J. Chem. Educ.* **2017**, *94*, 1752–1755.

Manuscript received: November 27, 2019
Revised manuscript received: January 29, 2020

© 2020 The Authors. Published by Wiley-VCH Verlag GmbH & Co. KGaA